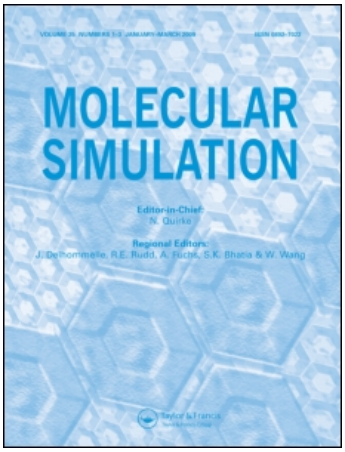

Molecular Simulation
Publication details, including instructions for authors and subscription information:
http://www.informaworld.com/smpp/title~content=t713644482

Molecular Dynamics Simulation of Collective Motions in Binary Liquids

N. Anento[a]; J. A. Padró[a]; O. Alcaraz[b]; J. Trullàs[b]
[a] Departament de Física Fonamental, Universitat de Barcelona, Barcelona, Spain [b] Departament de Física i Enginyeria Nuclear, Universitat Politècnica de Catalunya, Barcelona, Spain

Online publication date: 26 October 2010

To cite this Article Anento, N. , Padró, J. A. , Alcaraz, O. and Trullàs, J.(2003) 'Molecular Dynamics Simulation of Collective Motions in Binary Liquids', Molecular Simulation, 29: 6, 373 — 384
To link to this Article: DOI: 10.1080/0892702031000117171
URL: http://dx.doi.org/10.1080/0892702031000117171

Molecular Simulation, Vol. 29 (6–7), June 2003, pp. 373–384

Molecular Dynamics Simulation of Collective Motions in Binary Liquids

N. ANENTO[a], J.A. PADRÓ*, O. ALCARAZ[b] and J. TRULLÀS[b]

[a]*Departament de Física Fonamental, Universitat de Barcelona, Diagonal, 647. 08028 Barcelona, Spain;* [b]*Departament de Física i Enginyeria Nuclear, Universitat Politècnica de Catalunya, Jordi Girona Salgado, 1-3, B4-B5, 08034 Barcelona, Spain*

(Received July 2002; In final form November 2002)

Collective dynamic properties of different kind of binary liquid mixtures have been investigated by molecular dynamics simulation. The study includes both the longitudinal and the transverse current spectra in simple liquid alloys, 1:1 molten salts and liquid binary mixtures of neutral particles with an ionic-like structure. These systems were chosen as representative of binary liquids with different static structures in order to analyse the effects of structural ordering on the mechanisms of dynamic collective properties. The effect of the mass asymmetry between the two species in the mixture has been also discussed from the results for two different mass ratios for each kind of structure. Two length scales have been considered. On the one hand, the hydrodynamic scale (low wave numbers), where the modes for the partial currents of the two species are characterised by very close frequencies. On the other hand, the molecular scale (higher wave numbers), where the characteristic frequencies for the two species show noticeable differences. Vibrational concentration current modes (optic modes) have been found in neutral mixtures though their influence is rather weak, being the collective dynamic properties of this kind of systems dominated by the mass current modes (acoustic modes). On the contrary, in mixtures of charged particles such as molten salts the contribution of the concentration (charge) currents to the collective dynamics is important and optic modes can be characterised by a well-defined frequency for a wide range of wave numbers. It has been observed that heavy particles have a more relevant role on the mass current correlations whereas light particles play a dominant role on the concentration current correlations. The overall results for the three kinds of liquid mixtures analysed in this paper show that both the longitudinal and transverse current spectra are little dependent on the static structure of the system whereas marked differences are revealed when the particles in the system are either neutral or carry an electric charge.

Keywords: Molecular dynamics simulation; Dynamic structure factors; Transverse modes; Liquid mixtures

INTRODUCTION

The progress in the understanding of microscopic behaviour of liquids has been intimately related to the development of computer simulation and in the case of time-dependent properties to that of Molecular Dynamics (MD) method. MD is especially useful to analyse the dynamic collective properties of liquids at the intermediate $k-\omega$ region, which is the same that may be explored in neutron-scattering experiments. The collective dynamic properties of simple molten salts were studied in the early stages of computer simulation [1] whereas the interest for these properties in other binary liquids has more recently emerged as a result of the observation of "fast sound" modes associated with the motions of light particles in the Li_4Pb alloy [2]. Later studies have shown the existence of "slow sound" modes associated with the motions of heavy particles [3], which as the former have a non-hydrodynamic (kinetic) character. The transverse modes in binary liquids have been much less studied, which is probably due to the fact that they cannot be associated with any measurable magnitude. This fact turns the MD simulation into the only

*Corresponding author. E-mail: joan@ffn.ub.es

ISSN 0892-7022 print/ISSN 1029-0435 online © 2003 Taylor & Francis Ltd
DOI: 10.1080/0892702031000117171

source of "experimental" data for these collective properties [4,5].

The study of the collective dynamics in unicomponent liquids is normally based on the analysis of the intermediate scattering functions ($F(k,t)$)-the time correlations of density fluctuations in the reciprocal space-and corresponding spectra, the dynamic structure factors ($S(k,\omega)$). These functions, defined for spontaneous fluctuations in the equilibrium, are related to the response of the system when it is perturbed externally. The spectrum is directly related to measurements of coherent inelastic scattering of thermal neutrons with wavelengths ($\lambda = 2\pi/k$) around the interatomic distances [1]. At enough small k and ω (large time and space scales) $F(k,t)$ shows a decaying oscillatory behaviour. Thus, for a given wave number k, $S(k,\omega)$ has a relaxation peak centred at $\omega = 0$ (Rayleigh peak) that represents a thermal diffusive (non-vibrational) mode and two side peaks at $\omega = \pm ck$ (Brillouin peaks) that reflect the oscillatory behaviour of $F(k,t)$. The Brillouin peaks correspond to vibrational modes related to acoustic waves propagating with isothermal sound velocity c [1,6].

In simple binary liquids the partial intermediate scattering functions $F^{ab}(kt)$ at low k-values usually decay very slowly without any noticeable oscillation [7] whereas in other systems such as the Li_4Pb alloy or simple molten salts these functions show a fast decaying oscillatory behaviour. The peculiar behaviour of Li_4Pb was in principle attributed to the large mass ratio in this alloy [8,9] but recent MD studies have shown that this assumption is wrong and the Li_4Pb behaviour should be attributed to its rather ordered structure at short distances, which is analogous to the shells structure in 1:1 molten salts [10,11]. The slow decay of the $F^{ab}(k,t)$ functions is a problem for the calculation of the $S^{ab}(k,\omega)$ partial dynamic structure factors. Besides, the Rayleigh peak at $\omega = 0$ can be wide enough to hide the Brillouin peak at $\omega \neq 0$. Thus, it is useful to consider the partial longitudinal current correlation functions ($C_L^{ab}(k,\omega)$) [12], which are related to $S^{ab}(k,\omega)$ through [13]

$$C_L^{ab}(k,\omega) = (\omega/k)^2 S^{ab}(k,\omega) \qquad (1)$$

According to this relation, the $C_L^{ab}(k,\omega)$ functions do not show any peak at $\omega = 0$ while the peaks at high frequencies are enhanced and they become much more marked than the corresponding ones in $S^{ab}(k,\omega)$. So, the thermal diffusive contribution of density fluctuations will be removed from $C_L^{ab}(k,\omega)$ whereas the vibrational modes of density fluctuations will be enhanced.

The aim of this paper is to achieve a deeper understanding of the effects of structural ordering on the mechanisms of the dynamic collective properties in binary liquids. To this end the longitudinal and transverse current correlation functions for three kinds of systems with different structural features are compared. On the one hand, we considered two simple 1:1 molten salts (KCl and RbCl) with a regular alternation of concentric shells of oppositely charged ions (charge ordering). On the other hand, we chose liquid alloys ($Li_{0.5}Li_{0.5}$ and $Li_{0.5}Mg_{0.5}$) that shows the characteristic random structure of simple liquid mixtures. Finally we simulated, as intermediate systems, two ideal neutral ionic-like mixtures (RM1 and RM3) with a short-range structure similar to that of the molten salts. For each kind of system we have considered a mixture made up of species with the same, or very close, mass ($Li_{0.5}Li_{0.5}$, RM1 and KCl), which allow us to study solely the effects of structural ordering. Moreover, in order to analyse the influence of the difference of masses between the species in the mixtures, systems with a mass ratio about 3 were taken for each kind of structure ($Li_{0.5}Mg_{0.5}$, RM3 and RbCl). The study has been focussed on two sets of wave vectors that may be taken as representative of the "hydrodynamic" (low k) and "molecular" (higher k) length scales.

DESCRIPTION OF THE SIMULATIONS

Computation Details

Three kinds of equimolar ($x = 0.5$) binary liquids have been simulated by the ordinary MD method and considering usual periodic boundary conditions. In all cases the light particles in the mixture will be termed species "1" and the heavy particles species "2". The main characteristics of the simulated systems are the following:

(i) *Simple liquid alloys*: $Li_{0.5}Li_{0.5}$ at temperature $T = 725\,K$ and number density $\rho = 0.04213\,\text{Å}^{-3}$ and $Li_{0.5}Mg_{0.5}$ at temperature $T = 887\,K$ and number density $\rho = 0.040408\,\text{Å}^{-3}$. The former system is pure Li but assuming for the calculation of properties that half of particles belong to the species 1 and the other half to the species 2. The total number of particles was 668 in the case of $Li_{0.5}Li_{0.5}$ and 570 in the case of $Li_{0.5}Mg_{0.5}$. The interparticle forces were modelled according to the NPA potential [14], which reproduces the most representative features of liquid Li and Li-based alloys [6,10].

(ii) *Simple molten salts*: KCl at temperature $T = 1173\,K$ and ionic density $\rho = 0.0235\,\text{Å}^{-3}$ and RbCl at temperature $T = 1023\,K$ and number density $\rho = 0.0221\,\text{Å}^{-3}$. The systems were made up of 108 cations and 108 anions. The interionic forces were calculated using the effective Fumi-Tosi pair potentials reviewed by Sangster and

Dixon [15], which provide a realistic approach to the microscopic behaviour of molten alkali-halides. The Ewald method was used to compute the long-range coulomb interactions.

(iii) *Neutral ionic-like mixtures*: These ideal mixtures at temperature $T = 120\,\mathrm{K}$ and number density $\rho = 0.0326\,\mathrm{\AA}^{-3}$ were made up of 432 particles of each species. In the RM1 system both species have the same mass, $m_1 = m_2 = m_{\mathrm{Argon}}$, whereas in the RM3 system species 1 have the same mass $m_1 = m_{\mathrm{Argon}}$ but the mass of species 2 is $m_2 = 3m_1$. The interaction potential between particles of the same species was a repulsive soft sphere potential $V_{11} = V_{22}(r) = 4\varepsilon(\sigma_{11}/r)^6$, with $\varepsilon = 119.8\,\mathrm{K}$ and $\sigma_{11} = \sigma_{22} = 3.405\,\mathrm{\AA}$ whereas the interactions between particles of different species was a Lennard-Jones potential $V_{12}(r) = 4\varepsilon[(\sigma_{12}/r)^{12} - (\sigma_{12}/r)^6]$ with $\sigma_{12} = 0.65\sigma_{11}$. This relation between σ_{11} and σ_{12} was chosen on purpose to reproduce the local structure of 1:1 molten salts [11,12].

Structure of the Simulated Systems

The partial radial distribution functions between like ($g^{11}(r), g^{22}(r)$) and unlike ($g^{12}(r)$) particles were calculated during the MD runs and the results are gathered in Fig. 1. It should be noted that particles of species 1 and 2 are identical in RM1 whereas in RM3 the only difference is the atomic mass. Then, the structure between like particles is the same ($g_{11}(r) \equiv g_{22}(r)$). Because of the high symmetry between the two species in KCl the discrepancies between $g^{11}(r)$ and $g^{22}(r)$ are negligible for this system whereas only small differences may be observed for $Li_{0.5}Mg_{0.5}$. The partial structure factors ($S^{ab}(k)$, where $a = 1, 2$ and $b = 1, 2$) for neutral systems were obtained as the Fourier transforms of the corresponding $g^{ab}(r)$'s

$$S^{ab}(k) = \delta_{ab} + (N_a N_b)^{1/2} V^{-1} \int_0^\infty (g^{ab}(r) - 1) \times (\sin(kr)/kr) 4\pi r^2 \, \mathrm{d}r \quad (2)$$

whereas for simple molten salts were directly calculated during the MD runs

$$S^{ab}(\vec{k}) = (N_a N_b)^{-1/2} \times \left\langle \left[\sum_{la} \exp(-i\vec{k}\cdot\vec{r}_{la})\right]\left[\sum_{jb} \exp(-i\vec{k}\cdot\vec{r}_{jb})\right]\right\rangle \quad (3)$$

The $S^{ab}(k)$ results are plotted in Fig. 2. For the sake of simplicity, the $g^{ab}(r)$ and $S^{ab}(k)$ functions for $Li_{0.5}Li_{0.5}$ and RbCl have not been plotted in Figs. 1 and 2 since the structural features of these systems are analogous to those of $Li_{0.5}Mg_{0.5}$ and KCl, respectively.

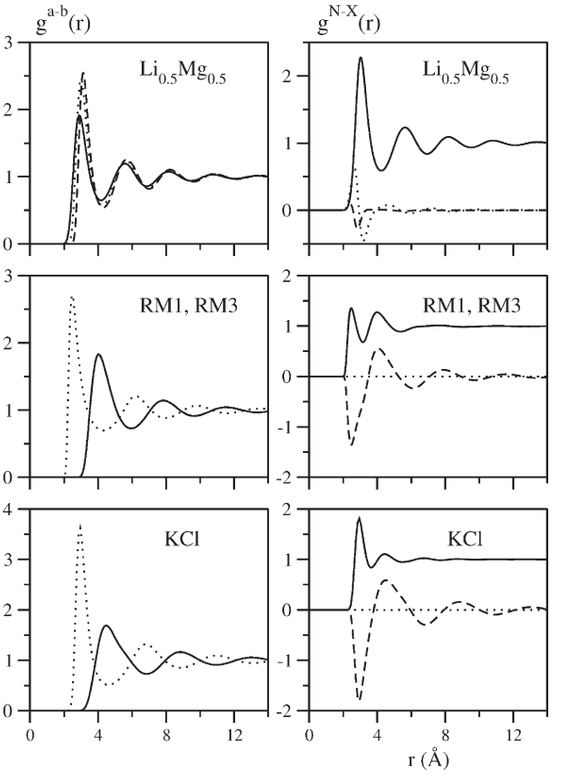

FIGURE 1 Radial distribution functions for different liquid mixtures. *Left side*. Partial pair correlation functions: $g^{11}(r)$ (full line), $g^{22}(r)$ (dashed line) and $g^{12}(r)$ (dotted line). *Right side*. Bathia-Thornton correlation functions obtained from the partial pair correlations following the definitions give in the text (Eqs. (4)–(6)): $g^{NN}(r)$ (full line), $g^{XX}(r)$ (dashed line) and $g^{NX}(r)$ (dotted line).

The $g^{ab}(r)$ functions in Fig. 1 show that the local structure of RM1 and RM3 is similar to that of molten salts such as KCl and RbCl. The maximums of the partial radial distribution functions for the like species are at the same position as the minimums for the unlike species and vice versa, which means that given a particle there is a regular alternation of concentric shells of different species (species ordering). However, this structure is very different from that of $Li_{0.5}Mg_{0.5}$, which corresponds to a random distribution of the two species in the mixture. The similarity between the structure of the RM1/RM3 systems and that of molten salts as KCl may be also clearly observed by comparing the partial structure factors between unlike species $S^{12}(k)$ (Fig. 2). For both RM1/RM3 and KCl, $S^{12}(k)$ shows a very marked negative minimum whereas for $Li_{0.5}Mg_{0.5}$ it shows a positive maximum at the equivalent position. Despite the similarity between the local structures in RM1/RM3 and KCl their origins are very different. In the former systems it is the result of the close packing of particles, being strongly dependent on the adequate choice of σ_{12} [11]. On the contrary, the structure of molten salts is

basically associated with the screening of electric charges to produce local neutrality.

The study of the structure of the binary liquids is frequently based on the Bathia-Thornton structure factors [16], which for equimolar mixtures can be written as

$$S^{\mathrm{NN}}(k) = \left[S^{11}(k) + S^{22}(k) + 2S^{12}(k)\right]/2 \qquad (4)$$

$$S^{\mathrm{NX}}(k) = \left[S^{11}(k) - S^{22}(k)\right]/2 \qquad (5)$$

$$S^{\mathrm{XX}}(k) = \left[S^{11}(k) + S^{22}(k) - 2S^{12}(k)\right]/2 \qquad (6)$$

$S^{\mathrm{NN}}(k)$ reflects the averaged structure of the system and represents the correlations between fluctuations in number density (irrespective of the species) while $S^{\mathrm{XX}}(k)$ is associated with the correlations between fluctuations in concentration. In the case of molten salts the XX correlations are usually termed ZZ since they are related to the charge density fluctuations. $S^{\mathrm{NX}}(k)$ for RM1/RM3 is zero (since $S^{11}(k) \equiv S^{22}(k)$ for these systems) whereas for KCl is negligible. $S^{\mathrm{NX}}(k)$ for $Li_{0.5}Mg_{0.5}$ show very small values (Fig. 2). The radial distribution functions $g^{\mathrm{NN}}(r)$, $g^{\mathrm{NX}}(r)$ and $g^{\mathrm{XX}}(r)$ corresponding to the structure factors defined above were also calculated and the results shown in Fig. 1. We notice that Eqs. (4)–(6) are those usually employed for 1:1 molten salts with X = Z while for equimolar binary alloys they are usually written as $S^{\mathrm{CC}}(k) = S^{\mathrm{XX}}(k)/4$ and $S^{\mathrm{NC}}(k) = S^{\mathrm{NX}}(k)/2$ [1,16].

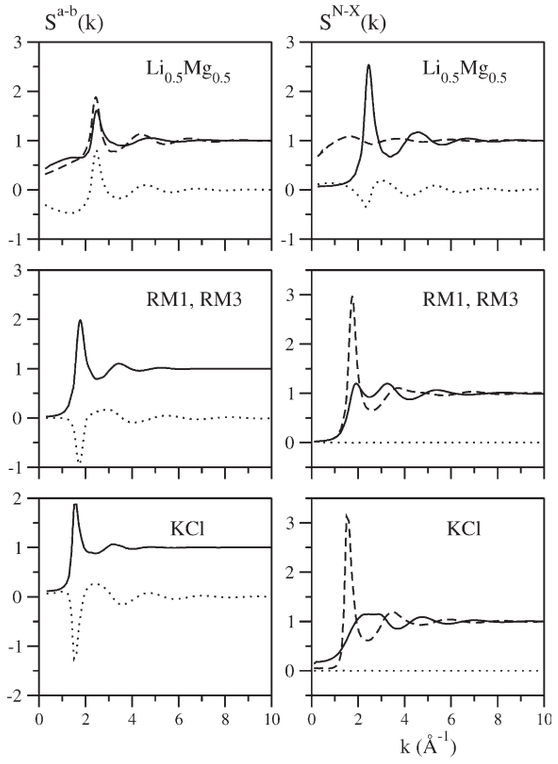

FIGURE 2 Static structure factors for different liquid mixtures. *Left side*. Partial structure factors: $S^{11}(k)$ (full line), $S^{22}(k)$ (dashed line) and $S^{12}(k)$ (dotted line). *Right side*. Bathia-Thornton structure factors defined in Eqs (4)–(6): $S^{\mathrm{NN}}(k)$ (full line), $S^{\mathrm{XX}}(k)$ (dashed line) and $S^{\mathrm{NX}}(k)$ (dotted line).

The results in Fig. 2 confirm that the structure of simple liquid mixtures of neutral particles such as $Li_{0.5}Li_{0.5}$ and $Li_{0.5}Mg_{0.5}$ is dominated by the NN (number density) correlations whereas the structure of systems with species ordering such as KCl and RbCl or RM1/RM3 is dominated by the XX correlations. Species ordering is clearly reflected in the first sharp peak of $S^{\mathrm{XX}}(k)$ and the first deep minimum of $S^{12}(k)$ at the same wave number. It should be noted that in the case of molten salts the values of the partial $S^{ab}(k)$ functions as $k \to 0$ are very small (and directly related to the isothermal compressibility [1]). This asymptotic behaviour is also shown by RM1/RM3 whereas $S^{ab}(k)$ for $Li_{0.5}Li_{0.5}$ and $Li_{0.5}Mg_{0.5}$ goes to values around 0.5 for like particles and around -0.5 for unlike particles as $k \to 0$.

Definitions of the Calculated Properties

The study carried out in this paper is based on the analysis of the longitudinal ($C_{\mathrm{L}}^{ab}(\vec{k},\omega)$) and transverse ($C_{\mathrm{L}}^{ab}(\vec{k},\omega)$) partial current spectra ($a = 1, 2$ and $b = 1, 2$; $1 \equiv$ light particles, $2 \equiv$ heavy particles), which are the time Fourier transforms ($C(k,\omega) = (2\pi)^{-1}\int C(k,t)\exp(i\omega t)\,\mathrm{d}t$) of the time current correlations calculated during the MD runs according to Refs. [1,13].

$$C_{\mathrm{L}}^{ab}(\vec{k},t) = N[N_aN_b]^{-1/2}\langle j_{\parallel}^{a}(\vec{k},t)\cdot j_{\parallel}^{b}(-\vec{k},0)\rangle \qquad (7)$$

$$C_{\mathrm{T}}^{ab}(\vec{k},t) = N[N_aN_b]^{-1/2}/2\langle j_{\perp}^{a}(\vec{k},t)\cdot j_{\perp}^{b}(-\vec{k},0)\rangle \qquad (8)$$

where $j_{\parallel}^{a}(\vec{k},t)$ and $j_{\perp}^{a}(\vec{k},t)$ are, respectively, the parallel and perpendicular component on the direction of $\vec{k}$ of the partial current

$$\vec{J}^{a}(\vec{k},t) = \sum\nolimits_{la}\vec{v}_{la}(t)\exp(-i\vec{k}\cdot\vec{r}_{la}(t)) \qquad (9)$$

It should be noted that $\vec{J}^{a}(\vec{k},t)$ is the space Fourier transform of the local current of species "a" in the real space $\vec{J}^{a}(\vec{R},t) = \sum_{la}\vec{v}_{la}(t)\delta(\vec{R} - \vec{r}_{la}(t))$, where $\vec{v}_{la}(t)$ and $\vec{r}_{la}(t)$ are the velocity and position of the particle "*la*" of species "*a*". Since we are considering isotropic fluids, the correlation functions are independent on the direction of $\vec{k}$ and they are determined as an average for different wave vectors with the same modulus k (wave number). The k-values considered for each system were chosen among those compatible with the respective periodic boundary condition i.e. $\vec{k} = (n_x, n_y, n_z)2\pi/L_{\mathrm{box}}$, where n_x, n_y and n_z are integers and L_{box} is the corresponding cubic box side.

We calculated also the longitudinal and transverse time correlations associated with

the mass ($\vec{J}^M(\vec{r},t) = m_1\vec{J}^1(\vec{r},t) + m_2\vec{J}^2(\vec{r},t)$) and concentration ($\vec{J}^\times(\vec{r},t) = x_2\vec{J}^1(\vec{r},t) - x_1\vec{J}^2(\vec{r},t)$) currents and corresponding spectra according to the definitions given in Ref. [16] (except normalising factors) with number fractions $x_1 = x_2 = 0.5$,

$$C_D^{\mathrm{MM}}(k,\omega) = \left[m_1^2 C_D^{11}(k,\omega) + m_2^2 C_D^{22}(k,\omega) + 2\mathrm{m_1 m_2} C_D^{12}(k,\omega)\right]/2 \quad (10)$$

$$C_D^{\mathrm{MX}}(k,\omega) = \left[m_1 C_D^{11}(k,\omega) - m_2 C_D^{22}(k,\omega) + (m_2 - m_1) C_D^{12}(k,\omega)\right]/2 \quad (11)$$

$$C_D^{\mathrm{XX}}(k,\omega) = \left[C_D^{11}(k,\omega) + C_D^{22}(k,\omega) - 2C_D^{12}(k,\omega)\right]/2 \quad (12)$$

where $D = \{\mathrm{L},\mathrm{T}\}$ indicates the longitudinal (L) or transverse (T) directions of the currents. The MM correlations reflect the averaged behaviour of the system so that in the limiting case of a mixture of two identical species they are equal to the correlation functions for the one-component liquid. The XX correlations (the charge current in molten salts) are associated with the relative motions of particles of different species. The longitudinal MM currents are related to the mass density fluctuations while the longitudinal XX currents are related to the concentration (charge density) fluctuations. It follows from Eqs. (10)–(12)

$$C_D^{11}(k,\omega) = \left[C_D^{\mathrm{MM}}(k,\omega) + m_1^2 C_D^{\mathrm{XX}}(k,\omega) + 2m_2 C_D^{\mathrm{MX}}(k,\omega)\right]/(2\bar{m}^2) \quad (13)$$

$$C_D^{12}(k,\omega = \left[C_D^{\mathrm{MM}}(k,\omega) - m_1 m_2 C_D^{\mathrm{XX}}(k,\omega) + 2(m_2 - m_1) C_D^{\mathrm{MX}}(k,\omega)\right]/(2\bar{m}^2) \quad (14)$$

$$C_D^{22}(k,\omega) = \left[C_D^{\mathrm{MM}}(k,\omega) + m_2^2 C_D^{\mathrm{XX}}(k,\omega) - 2m_1 C_D^{\mathrm{MX}}(k,\omega)\right]/(2\bar{m}^2) \quad (15)$$

where $\bar{m} = (m_1 + m_2)/2$ is the mean mass of particles for equimolar binary mixtures. Thus, the collective dynamics may be described by considering the mass and concentration currents instead of the partial currents.

It can be shown for both the longitudinal and the transverse currents that the initial values of the partial cross-correlations ($a \neq b$) are equal to zero and the initial values of the partial autocorrelations ($a \neq b$) are equal to $k_B T/m_a$, i.e. $\int C_D^{ab}(k,\omega)d\omega = C_D^{ab}(k,t=0) = \delta_{ab}k_B T/m_a$ (where k_B is the Boltzmann's constant) [13]. Thus, the area under a current autocorrelation spectrum does not change with k. For the sake of comparison the time correlation functions shown in this paper were normalised according to Ref. [17]

$$C_D^{\alpha\beta}(k,t) = \frac{C_D^{\alpha\beta}(k,t)}{\left[C_D^{\alpha\beta}(k,t=0)\cdot C_D^{\alpha\beta}(k,t=0)\right]^{1/2}} \quad (16)$$

where the $C_D^{\alpha\beta}(k,t)$ functions refers to both the partial "ab" correlations defined in Eqs. (7) and (8) and the "MX" correlations defined in Eqs. (10)–(12). This normalisation factor was chosen so that $\int C_D^{\alpha\alpha}(k,\omega)\mathrm{d}\omega = 1$.

RESULTS

In order to analyse the influence of the structure on the dynamic collective properties it is useful to remove the effects of other factors as the mass differences between particles of distinct species. Thus, the results for mixtures of species with the same or very close masses are presented ("Mixtures with Similar Masses ($m_2/m_1 \cong 1$)" Section) separately from those for systems with different masses ("Mixtures with Different Masses ($m_2/m_1 \cong 3$)" Section). For each system we discuss the results for two length scales. At the hydrodynamic regime (low wave numbers) the modes for the partial currents of the two species are characterised by very close frequencies. At the molecular regime (higher wave numbers) the characteristic features of the distinct species would become apparent when $m_1 \neq m_2$. The wave numbers for the discussion of the results at each regime were chosen so that the normalised value $\bar{k} = k/k_{\max}$ is similar for the three systems. $k_{\max}$ is the wave number corresponding to the first maximum of the static structure factor between like particles (see Table I and Fig. 2). Though the discussions in this paper are only based on the findings at two wave numbers for each system we have obtained also results at other wave numbers. So, it has been checked that according to earlier studies [10–12] the transition between the hydrodynamic and molecular regimes is continuous and strongly dependent on the mass differences between the two species in the mixture.

Mixtures with Similar Masses ($m_2/m_1 \cong 1$)

In this section, we discuss the influence of the structural order on the current correlations from

TABLE I MD simulation parameters and wave numbers corresponding to the S(k) first maximums for the studied systems

	$Li_{0.5}Li_{0.5}$	$Li_{0.5}Mg_{0.5}$	RM1/RM3	KCl	RbCl
ρ (part./Å^3)	0.04213	0.040408	0.0326	0.0235	0.0221
T(K)	725	887	120	1173	1023
k_{max}(Å^{-1})	2.44	2.45	1.76	1.6	1.6

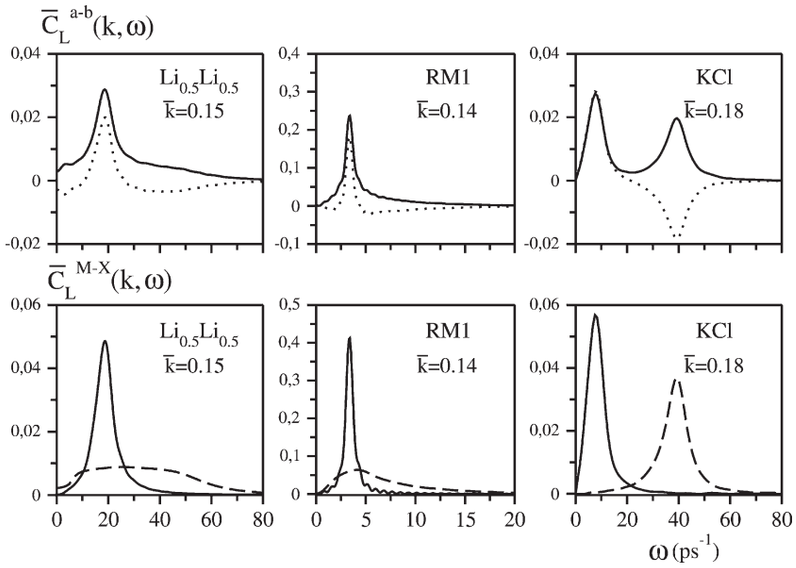

FIGURE 3 Normalised longitudinal current spectra at hydrodynamic scale ($\bar{k} = k/k_{max} \approx 0.15$) for liquid mixtures with similar masses ($m_2/m_1 \approx 1$). *Above*: Partial spectra for like ($\tilde{C}_L^{11}(k,\omega)$, full line) and unlike ($\tilde{C}_L^{12}(k,\omega)$, dotted line) particles. *Below*: Mass ($\tilde{C}_L^{MM}(k,\omega)$, full line) and concentration ($\tilde{C}_L^{XX}(k,\omega)$, dashed line) spectra.

the results for mixtures where the two species do not show significant differences. In $Li_{0.5}Li_{0.5}$ the two species are identical, being a tag in a half part of the particles the only difference between them. In RM1 the two species are also identical and the interactions between like particles are the same though different from those between unlike particles. Because of the symmetry between the two species in these mixtures, $C_D^{11}(k,\omega) = C_D^{22}(k,\omega)$ and then $C_D^{MX}(k,\omega) = 0$ (see Eq. (11)). In KCl the mass of anions and cations is very close though not exactly the same, being the only significant difference the sign of their electric charges. Thus, the discrepancies between the current correlation functions between the like particles (11 and 22) are very small and the MX correlations almost negligible. For the sake of clarity the 22 and the MX correlations have not been plotted in Figs. 3–6.

Hydrodynamic Regime

The partial longitudinal current spectra ($C_L^{ab}(k,\omega)$) for the three analysed systems show two relevant

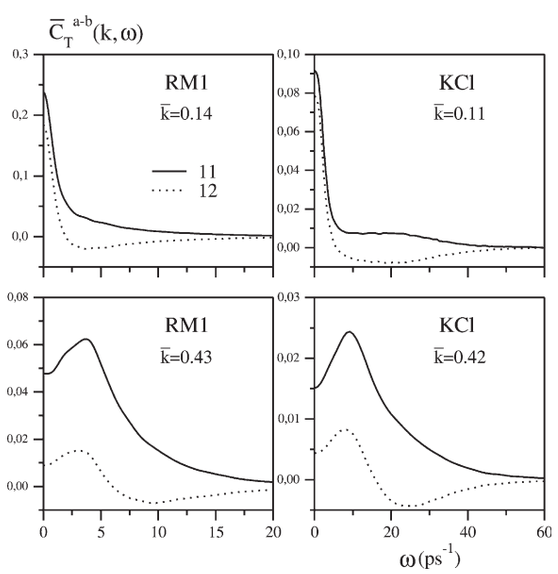

FIGURE 4 Normalised partial transverse current spectra for liquid mixtures with similar masses ($m_2/m_1 \approx 1$) : $\tilde{C}_T^{11}(k,\omega)$ (full line) and $\tilde{C}_T^{12}(k,\omega)$ (dotted line). *Above*: Hydrodynamic scale ($\bar{K} = K/K_{max} \approx 0.15$). *Below*: Molecular scale ($\bar{k} = k/k_{max} \approx 0.45$).

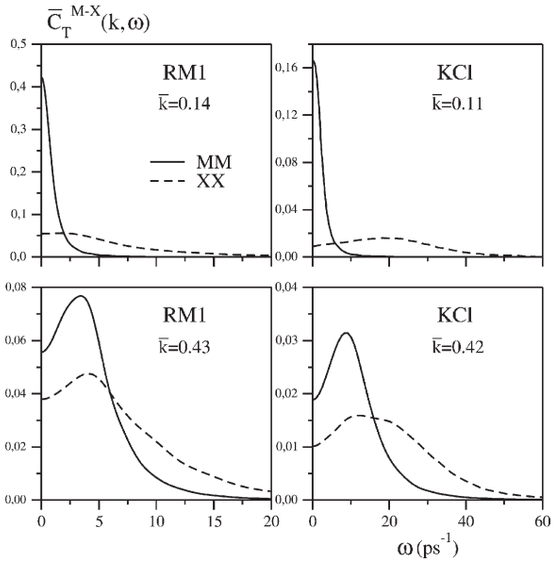

FIGURE 5 Normalised mass ($\tilde{C}_T^{MM}(k,\omega)$, full line) and concentration ($\tilde{C}_T^{XX}(k,\omega)$, dotted line) transverse current spectra for liquid mixtures with similar masses ($m_2/m_1 \approx 1$). *Above*: Hydrodynamic scale ($\bar{k} = k/k_{max} \approx 0.15$). *Below*: Molecular scale ($\bar{k} = k/k_{max} \approx 0.45$).

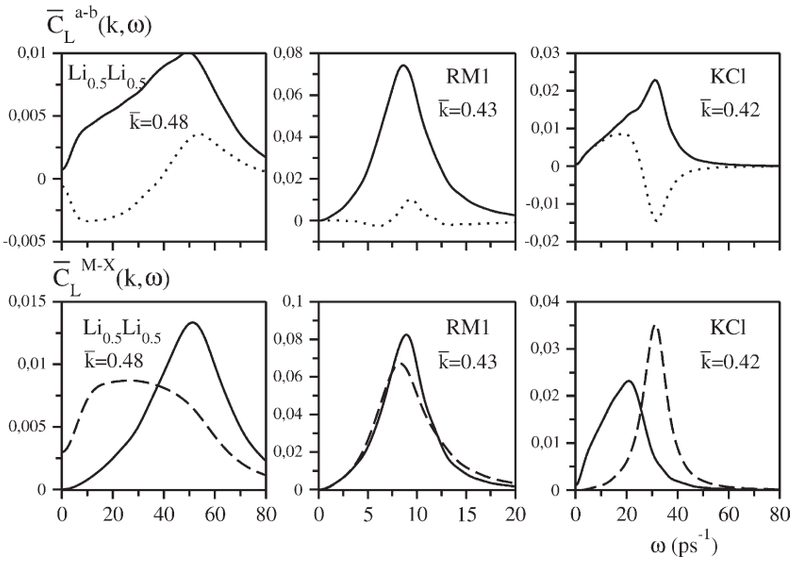

FIGURE 6 Normalised longitudinal current spectra at molecular scale ($\bar{k} = k/k_{max} \approx 0.45$). for liquid mixtures with similar masses ($m_2/m_1 \approx 1$). *Above*: Partial spectra for like ($\bar{C}_L^{11}(k,\omega)$, full line) and unlike ($\bar{C}_L^{12}(k,\omega)$, dotted line) particles. *Below*: Mass ($\bar{C}_L^{MM}(k,\omega)$,full line) and concentration ($\bar{C}_L^{XX}(k,\omega)$, dashed line) spectra.

frequencies (see the upper frames of Fig. 3). The lower frequency may be identified through a sharp peak that is also present in the corresponding $C_L^{MM}(k,\omega)$ functions. As with unicomponent liquids [1,6], the presence of the MM peak denotes a vibrational mode usually termed longitudinal acoustic (LA) mode since it is associated with propagating sound waves. The frequency corresponding to this peak, which we refer as $\omega_{LA}(k)$, decreases linearly with the wave number and the ratio $\omega_{LA}(k)/k$ yields the velocity of propagation of sound through the system. The higher frequency in the partial current spectra for like particles appears as a pronounced peak in $C_L^{11}(k,\omega)$ for KCl and a slight shoulder in $C_L^{11}(k,\omega)$ for both $Li_{0.5}Li_{0.5}$ and RM1. These features should be attributed to concentration current modes as shown by the corresponding $C_L^{XX}(k,\omega)$ functions, which present a marked peak for KCl and a broad maximum for $Li_{0.5}Li_{0.5}$ and RM1 at the same positions as those in $C_L^{11}(k,\omega)$. Moreover, $C_L^{12}(k,\omega)$ presents a minimum (much more marked for KCl) with negative values at the same interval of frequencies. This indicates that these high frequency modes should be associated with vibrational motions in opposite directions of particles of different species. In the case of charged particles these modes are usually termed longitudinal optic (LO) modes, and we refer as $\omega_{LO}(k)$ the frequencies of the corresponding peaks.

It should be emphasized that results in Fig. 3 show that the LO modes have a relevant contribution to the collective dynamic properties of KCl, whereas in the case of $Li_{0.5}Li_{0.5}$ and RM1 the contribution of these modes is significantly lower and hardly visible in the partial longitudinal current spectra. These differences indicate that the role played by the concentration fluctuations become much more important when the particles are charged. It is well known that neutral binary mixtures cannot support the propagation of concentration fluctuations at the hydrodynamic limit $k = 0$ [1,18] whereas theoretical studies of charged liquid mixtures within the framework of generalised hydrodynamics have proved the existence of charge-density fluctuations of high frequency at long length scales [1]. This has been corroborated by experimental infrared reflectivity data for molten LiF [19]. These findings suggest that the characteristics of longitudinal modes at high frequencies are mainly determined by the electrical nature of particles. This may be attributed to the fact that in coulomb systems the concentration fluctuations and corresponding longitudinal currents arise from the tendency to produce local neutrality, which is absent in non-charged systems. Thus, although the structure of both RM1 and KCl present a very similar species ordering their collective dynamic properties show marked qualitative differences.

It has been corroborated that the changes of $C_L^{MM}(k,\omega)$ with k are analogous to those of $C_L(k,\omega)$ for unicomponent liquids. So, for the three systems studied the main peak of $C_L^{MM}(k,\omega)$ become sharper as $k \to 0$ and $\omega_{LA}(k)$ decreases linearly with k. Moreover, it has been checked that $C_L^{XX}(k,\omega)$ for the non-charged mixtures becomes markedly lower and wider as k decreases, which is consistent with the absence of LO modes at the hydrodynamic limit [18]. On the contrary, the width and height of the $C_L^{XX}(k,\omega)$

peak for molten KCl remains almost constant as k goes to zero and $\omega_{LO}(k)$ increases slightly up to a finite value as $k \to 0$. This confirms that molten salt supports LO modes at the hydrodynamic limit [1].

We turn next to transverse currents that, unlike longitudinal currents, are not related to the density fluctuations. Moreover the initial values of their spectra are not zero. The results for $Li_{0.5}Li_{0.5}$ have not been represented in Figs. 4 and 5 since they do not show significant differences in relation to those for RM1. The partial transverse current spectra for RM1 and KCl at wave numbers corresponding to the hydrodynamic regime are plotted in the upper frames of Fig. 4. Unlike with the longitudinal spectra, the shapes of the transverse spectra for neutral and charged systems look quite similar. It may be noticed in Fig. 4 that both $C_T^{11}(k,\omega)$ and $C_T^{12}(k,\omega)$ decay monotonically at low frequencies, as typical of diffusive processes. However, $C_T^{11}(k,\omega)$ shows a slight shoulder around the same frequency interval for which $C_T^{12}(k,\omega)$ has a minimum with negative values. This fact reveals that, as with longitudinal modes, there are transverse modes associated with vibrational motions in opposite directions of particles of distinct species. Moreover $C_T^{XX}(k,\omega)$ shows a broad maximum about the same interval of frequencies (see the upper frames of Fig. 5). This shows that the shoulders in $C_T^{11}(k,\omega)$ should be attributed to vibrational transverse concentration current modes that according to the usual nomenclature for molten salts are termed transverse optic (TO) modes.

It may be observed in the upper frames of Fig. 5 that $C_T^{MM}(k,\omega)$ decays monotonically without any shoulder at high frequencies. In agreement with hydrodynamic predictions for simple liquids, these results corroborate that transverse sound waves cannot propagate through liquid mixtures since these systems are not able to support shear stress at macroscopic scales. It has been verified that molten KCl support TO modes as $k \to 0$ and the limiting values of $\omega_{LO}(k)$ and $\omega_{TO}(k)$ satisfy the Lyddane-Sachs-Teller relation $\omega_{LO}^2(0) - \omega_{TO}^2(0) = \omega_p^2$, where ω_p is the plasma frequency [1].

Molecular Regime

The results for the longitudinal current spectra at wave numbers that are expected to correspond to the molecular regime are shown in Fig. 6. It should be noted that the peaks of $C_L^{11}(k,\omega)$, $C_L^{12}(k,\omega)$ and $C_L^{MM}(k,\omega)$ for both $Li_{0.5}Li_{0.5}$ and RM1 are lower and wider than those at the hydrodynamic region in Fig. 3 (notice that the scales of these figures are different). On the contrary, for KCl the height and width of these functions are similar at the two regions. The molecular regime has been defined as that for which the distinctive features of the two species become relevant. However, because of the great symmetry between the two species in the systems considered in this section the 11 spectra are very close (or identical) to the 22 spectra and the differences expected at molecular scales only will be noticeable for systems with $m_2 > m_1$ discussed in the next section. The results in the lower frames of Fig. 6 show that the differences between $C_L^{MM}(k,\omega)$ and $C_L^{XX}(k,\omega)$ for a given system are smaller than those in Fig. 3, which suggest that the frequencies for the mass and concentration longitudinal modes tend to be closer at shorter length scales. Nevertheless, clear differences between these modes can be noticed in $C_L^{12}(k,\omega)$ for $Li_{0.5}Li_{0.5}$ and KCl that shows a minimum and a maximum, which correspond to LO and LA modes, respectively. These modes are also present but hardly visible in $C_L^{11}(k,\omega)$. Since for RM1 the frequencies associated with the LA and LO modes are practically equal ($\omega_{LA}(k) \approx \omega_{LO}(k)$) the corresponding maximum and minimum in $C_L^{12}(k,\omega)$ overlap and only a low resulting maximum may be distinguished.

The resulting transverse current correlation functions for k-values representative of molecular scales are displayed in the lower frames of Figs. 4 and 5. It should be noted the similarity between the results for neutral systems and molten salts. Both $C_T^{11}(k,\omega)$ and $C_T^{12}(k,\omega)$ in Fig. 4 show a side peak that is also present in $C_T^{MM}(k,\omega)$ of Fig. 5. Besides, it has been verified that the frequency corresponding to this peak ($\omega_{TA}(k)$) decreases linearly with k. The $C_T^{MM}(k,\omega)$ results are consistent with those $C_T(k,\omega)$ in dense unicomponent liquids, where the existence of vibrational transverse modes was also observed at the molecular regime. These modes, which are usually termed "shear" modes, are attributed to viscoelastic effects [1]. It may be also observed in Fig. 5 that $C_T^{XX}(k,\omega)$ shows a slight shoulder at a frequency $\omega_{TO}(k)$ somewhat higher than $\omega_{TA}(k)$ ($\omega_{TO}(k) \approx 10\,ps^{-1}$ for RM1 and $\omega_{TO}(k) \approx 25\,ps^{-1}$ for KCl). It is interesting to note that the presence of a shoulder in $C_T^{XX}(k,\omega)$ is corroborated by $C_T^{12}(k,\omega)$, which shows a minimum with negative values at $\omega_{TO}(k)$. As could be expected from the results for longitudinal modes, the $C_T^{12}(k,\omega)$ functions have also a maximum at $\omega_{TA}(k)$. The partial transverse spectra in the free particle limit ($k \to \infty$) show a Gaussian shape centred at $\omega = 0$ [13] that corresponds to a single-particle diffusive dynamics without vibrational transverse modes. Thus, the TA modes only occur at molecular scales. The TO modes for mixtures of non-charged particles are also restricted to molecular scales whereas for ionic systems the TO modes also are present at the hydrodynamic regime.

Mixtures with Different Masses ($m_2/m_1 \cong 3$)

In this section, we discuss the effects on the dynamic collective properties induced by the difference of

mass between the particles of distinct species. To this end we have considered three systems of similar characteristics to those analysed in the previous section but with a larger mass ratio, i.e. $Li_{0.5}Mg_{0.5}$ with $m_2/m_1 \cong 3.5$, RM3 with $m_2/m_1 \equiv 3$ and RbCl with $m_2/m_1 \cong 2.4$ (it should be noted that Li is species 1 in $Li_{0.5}Mg_{0.5}$ whereas Rb^+ is species 2 in RbCl).

Hydrodynamic Regime

According to earlier findings [12], the higher is the ratio of the masses of species in the mixture the lower are the values of k for which the transition between hydrodynamic and molecular regimes is observed. Thus the wave numbers chosen to characterise the hydrodynamic regime in Figs. 7–9 are lower than those in Figs. 3–5. Unlike for systems with $m_2/m_1 \cong 1$, for the systems analysed in this section $C_D^{11}(k,\omega)$ is in general different of $C_D^{22}(k,\omega)$ and $C_D^{MX}(k,\omega)$ can show noticeable deviations from zero. However, at the hydrodynamic regime the coupling between the mass and concentration currents is very weak ($C_D^{MX}(k,\omega) \approx 0$). This corroborates the suitability of the M–X set of functions to analyse these length scales (it should be noticed that within the set of partial functions the cross correlations $C_L^{12}(k,\omega)$ are always important).

As with systems where $m_1 \approx m_2$, the partial longitudinal spectra show a sharp peak at the same frequency as that of $C_L^{MM}(k,\omega)$ (Fig. 7) that may be associated with propagating acoustic modes. These findings reflect a strong coupling between the dynamics of the two species at hydrodynamic scales. The existence of high frequency modes associated with concentration fluctuations (optic modes) may be noticed also in Fig. 7. $C_L^{XX}(k,\omega)$ for both $Li_{0.5}Mg_{0.5}$ and RM3 shows a broad maximum that produces a slight shoulder in the corresponding $C_L^{11}(k,\omega)$ and $C_L^{22}(k,\omega)$ functions. Although the shoulder is almost imperceptible in the second function the effect of these modes on the partial currents is confirmed by the negative minimum of $C_L^{12}(k,\omega)$ at the same frequencies. In the case of RbCl the optic modes are more significant and the peaks of $C_L^{11}(k,\omega)$, $C_L^{22}(k,\omega)$ and $C_L^{XX}(k,\omega)$ as well as the minimum of $C_L^{12}(k,\omega)$ are much more marked. These results suggest the suitability of using the acoustic and optic modes to describe the collective dynamics of liquid mixtures at low wave numbers. Nevertheless it should be noted that in the case of mixtures of neutral particles the optic modes vanishes at the hydrodynamic limit being the collective dynamic of these systems dominated by the acoustic modes.

The partial transverse current spectra for like particles ($C_T^{11}(k,\omega)$ and $C_T^{22}(k,\omega)$) show a slight shoulder at high frequencies (see the upper frames of Fig. 8). Both the shallow minimum in $C_T^{12}(k,\omega)$ and the broad maximum in $C_T^{XX}(k,\omega)$ at the same ω-interval (upper frames of Fig. 9) allow us to associate these features with transverse optic modes. As with the longitudinal currents these modes should be mainly attributed to light species. According to the results in Figs. 8 and 9 the larger

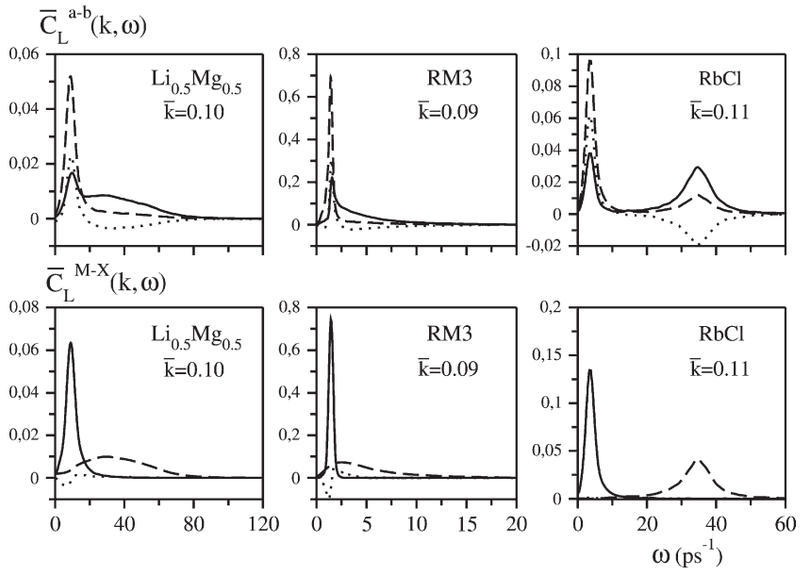

FIGURE 7 Normalised longitudinal current spectra at hydrodynamic scale ($\bar{k} = k/k_{max} \approx 0.1$) for liquid mixtures with different masses ($m_2/m_1 \approx 3$). *Above*. Partial spectra: $\bar{C}_L^{11}(k,\omega)$ (full line), $\bar{C}_L^{22}(k,\omega)$ (dashed line) and $\bar{C}_L^{12}(k,\omega)$ (dotted line). *Below*. Mass-concentration spectra: $\bar{C}_L^{MM}(k,\omega)$ (full line), $\bar{C}_L^{XX}(k,\omega)$ (dashed line) and $\bar{C}_L^{MX}(k,\omega)$ (dotted line).

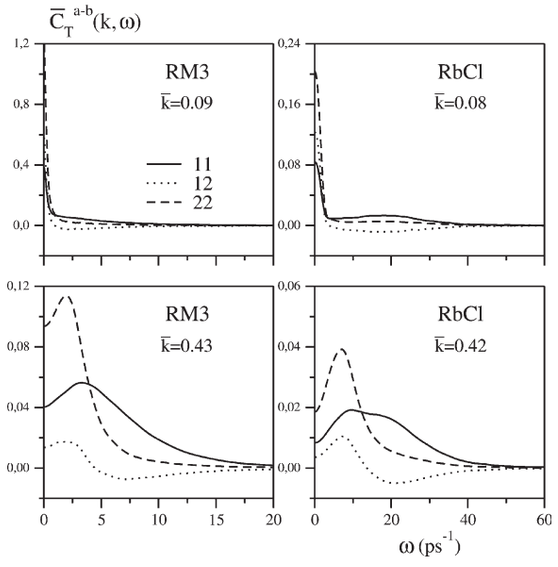

FIGURE 8 Normalised partial transverse current spectra for liquid mixtures with different masses ($m_2/m_1 \approx 3$) : $\tilde{C}_T^{11}(k,\omega)$ (full line), $\tilde{C}_T^{22}(k,\omega)$ (dashed line) and $\tilde{C}_T^{12}(k,\omega)$ (dotted line). *Above*: Hydrodynamic scale ($\bar{k} = k/k_{max} \approx 0.1$). *Below*: Molecular scale ($\bar{k} = k/k_{max} \approx 0.45$).

contribution to $C_T^{MM}(k,\omega)$ come from the functions related to the heavy particles and this contribution is purely diffusive.

Molecular Regime

The longitudinal current spectra plotted in Fig. 10 show a noticeable decoupling between the dynamics of the two species at molecular scale, which can be characterised by two different frequencies for a given wave number. The frequency corresponding to the maximum for light particles, $\omega_L^{11}(k)$ is higher than that for heavy particles, $\omega_L^{22}(k)$. In the case of neutral liquids the ratios $\omega_{LA}(k)/k$ for light and heavy particles are higher and lower, respectively, than the sound velocity given by $\omega_{LA}(k)/k$ at the hydrodynamic region. For this reason these modes were termed "fast sound" and "slow sound", respectively. Nevertheless, such modes cannot be considered as propagating sound modes since they are local modes (with rather short range) of kinetic character [10–12]. It should be pointed out that the values of $\omega_L^{11}(k)/k$ and $\omega_L^{22}(k)/k$ become the same and equal to $\omega_{LA}(k)/k$ at hydrodynamic length scales.

The partial current spectra for like particles ($C_L^{11}(k,\omega)$ and $C_L^{22}(k,\omega)$) show a marked maximum and a slight shoulder at about the same ω-intervals as the maximum and minimum of $C_L^{12}(k,\omega)$, respectively. According to the findings discussed in earlier paragraphs one could associate them with LA and LO modes. However, now the mass asymmetry reveals that the set of mass and concentration currents is not a very suitable set of functions to analyse the molecular regime. At molecular scale $C_L^{MX}(k,\omega)$ does not vanishes, which reflects that the mass and concentration currents are correlated. Moreover, in general $C_L^{MM}(k,\omega)$ and $C_L^{XX}(k,\omega)$ do not present a single well-defined peak so that the frequencies $\omega_{LA}(k)$ and $\omega_{LO}(k)$ cannot be unambiguously determined. This is clearly illustrated by $C_L^{XX}(k,\omega)$ for RM3 that shows two noticeable maximums (Fig. 10). Thus the set of partial currents seems to be more suitable to analyse the molecular regime since both $C_L^{11}(k,\omega)$ and $C_L^{22}(k,\omega)$ show a characteristic vibrational mode and $C_L^{12}(k,\omega)$ practically vanishes. Although the mass and concentration currents for RbCl at $\bar{k} = 0.44$ show well defined acoustic and optic modes we have checked that the results at $\bar{k} > 0.5$ resemble to those for RM3 and $Li_{0.5}Mg_{0.5}$, which suggests that for simple molten salts the molecular regime is not fully achieved at $\bar{k} = 0.42$.

The results for the transverse currents (lower frames of Figs. 8 and 9) are quite similar to those for mixtures with $m_2/m_1 \cong 1$, except that the low-frequency side peak attributed to shear modes is not at the same position for $C_T^{11}(k,\omega)$ and $C_T^{22}(k,\omega)$. As for longitudinal currents, the frequency corresponding to the maximum for light particles is higher than that for heavy particles. Moreover, the current spectra for heavy and light particles are quite similar to the mass and concentration current spectra, respectively.

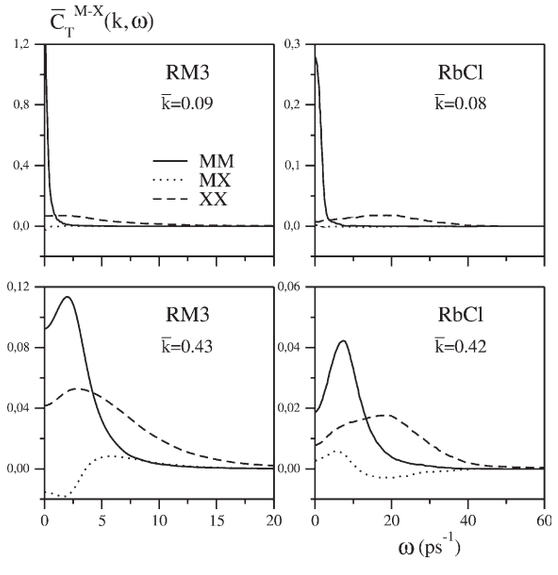

FIGURE 9 Normalized mass-concentration transverse current spectra for liquid mixtures with different masses ($m_2/m_1 \approx 3$) : $\tilde{C}_T^{MM}(k,\omega)$ (full line), $\tilde{C}_T^{XX}(k,\omega)$ (dashed line) and $\tilde{C}_T^{MX}(k,\omega)$ (dotted line). *Above*: Hydrodynamic scale ($\bar{k} = k/k_{max} \approx 0.15$). *Below*: Molecular scale ($\bar{k} = k/k_{max} \approx 0.45$).

CONCLUDING REMARKS

According to the findings discussed along this paper the current spectra for different kind of binary liquid

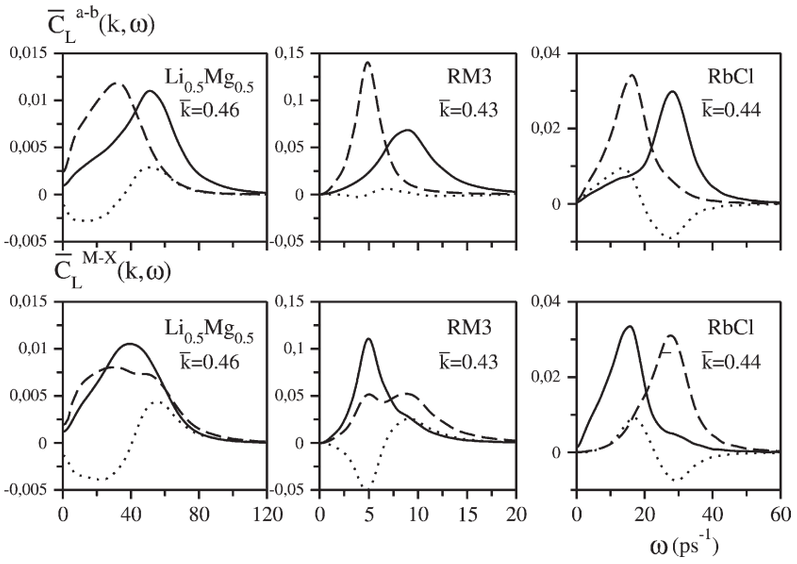

FIGURE 10 Longitudinal current spectra at molecular scale ($\bar{k} = k/k_{max} \approx 0.45$) for liquid mixtures with different masses ($m_2/m_1 \approx 3$). *Above*. Partial spectra: $\bar{C}_L^{11}(k,\omega)$ (full line), $\bar{C}_L^{22}(k,\omega)$ (dashed line) and $\bar{C}_L^{12}(k,\omega)$ (dotted line). *Below.* Mass-concentration spectra: $\bar{C}_L^{MM}(k,\omega)$ (full line), $\bar{C}_L^{XX}(k,\omega)$ (dashed line) and $\bar{C}_L^{MX}(k,\omega)$ (dotted line).

mixtures show some common qualitative trends. Both the longitudinal and transverse partial current spectra at hydrodynamic scales (low wave numbers k) present two characteristic frequencies. The lower is associated with mass current modes (acoustic) while the higher is associated with concentration current modes (optic). The transverse mass current spectra at low k only show a maximum at $\omega = 0$ (diffusive mode) whereas at molecular scales (higher k) they present a side peak, which reflects the existence of vibrational transverse acoustic modes (shear modes) that vanishes as k approaches to the free particle regime ($k \to \infty$). It has been observed that the currents for the heavier particles have a prominent role on the mass current correlations while the currents for the light particles have a prominent role on the concentration currents correlations.

Besides the resemblances, significant discrepancies have been found between the results for the mixtures of different kinds. At low wave numbers, the contribution of the concentration current modes to the dynamics of binary liquid mixtures of neutral particles, such as simple Li-based alloys or RM1/RM3 ideal mixtures, is rather weak. Thus the collective dynamic properties of these systems at large length scales are dominated by the mass (acoustic) modes and these systems do not support concentration fluctuations in the hydrodynamic limit ($k = 0$). On the contrary, in liquid mixtures of charged particles, such as simple molten salts, the contribution of the concentration fluctuations (actually charge density fluctuations) is relevant and the optic modes can be characterised by a well-defined frequency for a wide range of wave numbers including $k = 0$. At higher wave numbers (molecular regime) the peaks of both the partial and the mass longitudinal current spectra for non-charged systems are much lower and wider than those at the hydrodynamic region but the height and width of these functions for simple molten salts are similar at the two wave numbers presented in this work. This indicates that the transition between the hydrodynamic and molecular regimes for molten salts occurs at shorter length scales than for non-charged mixtures.

The asymmetry between the masses of species in the mixture has a more significant influence on the current spectra at short length scales since at long length scales the partial current modes of the two species are characterised by the same two frequencies, which are associated with mass and concentration modes, respectively. At molecular scales the partial currents may be characterised by a simple vibrational mode with a frequency that is higher for light particles than for the heavy. The mass and concentration currents are a very suitable set of functions to analyse the collective particle dynamics of liquid mixtures at the hydrodynamic regime but not at the molecular regime since, in general, the spectra of these functions do not present a well-defined single peak at short length scales. At the molecular regime the frequency corresponding to the maximum of the mass current spectra, if it can be identified, is lower than that of the concentration current spectra. These frequencies are quite close to the characteristic frequencies from the partial currents corresponding to the heavy and light particles, respectively.

We want to emphasize that the collective dynamics properties, as characterized by the current spectra, of

KCl/RbCl are markedly different from those of RM1/RM3 despite their structures are very similar, showing a noticeable species ordering. On the contrary, the results for $Li_{0.5}Li_{0.5}/Li_{0.5}Mg_{0.5}$ and RM1/RM3 show a high resemblance despite the large differences in their structures. This indicates that the collective dynamics of liquid mixtures is weakly influenced by the static structure of the systems whereas marked differences are revealed when the particles in the system are either neutral or carry an electric charge. This fact is somewhat surprising since recent MD studies [11] suggested that the characteristics of collective properties could be significantly influenced by the structure of the mixture. It was shown that the slow decay of the partial intermediate scattering functions $F^{ab}(k, t)$ in simple liquid mixtures such as $Li_{0.5}Li_{0.5}/Li_{0.5}Mg_{0.5}$ becomes markedly damped in mixtures as RM1/RM3, which have a shells structure resembling that of 1:1 molten salts. Nevertheless, according to the present findings the influence of the structure on the density fluctuations is not transferred to the current spectra. It should be noted that the Rayleigh peak of $S^{ab}(k,\omega)$ at $\omega = 0$, which reflects the long time decay of the $F^{ab}(k,t)$ functions, is not present in the partial longitudinal current spectra (see Eq. (1)). Then, the static structure play an important role on the relaxation of the partial density fluctuations related to thermal diffusive processes but not on the vibrational modes. The partial $S^{ab}(k)$ structure factors at $k \to 0$ go to very small values for liquid mixtures with species ordering but to relatively high values for mixtures with random distribution of the two species. Taking into account that $S^{ab}(k) = F^{ab}(k, t = 0)$, the $F^{ab}(k,t)$ functions with a slow time decay that hides the vibrational modes correspond to systems with high $S^{ab}(k)$ initial values whereas the damped oscillations of $F^{ab}(k,t)$ are only observable for systems with very small $S^{ab}(k)$ initial values.

The discrepancies between the collective dynamics of liquids made up of neutral and charged particles may be related to the different microscopic mechanisms that determine their structural and time dependent properties. It should be remembered that the shells distribution in 1:1 molten salts is the result of the screening of electric charges to produce local neutrality, while in RM1/RM3 is only the result of close packing and strongly dependent on the adequate choice of the parameter σ_{12} for the interaction potential between particles of different species. The time evolution of concentration fluctuations in molten salts should be mainly attributed to relatively large "restoring forces" to produce local neutrality, which are the result of strong electric fields induced by charge fluctuations. However, in neutral liquids the time evolution of concentration fluctuations is due to diffusion processes which effects have a much lower intensity. The findings discussed in this paper suggest that the mechanisms associated with the acoustic modes in both neutral mixtures and molten salts within the hydrodynamic region are quite similar and essentially related to packing effects.

Acknowledgements

The financial supports from the DGICYT of the Spanish government (Grant BFM2000-0596-C03-01) and the CIRIT of the "Generalitat de Catalunya" (Grant 2001SGR-00222) are gratefully acknowledged.

References

[1] Hansen, J.P. and McDonald, I.R. (1986) *Theory of Simple Liquids* (Academic Press, London).
[2] Bosse, J., Jacucci, G. and Schirmacher, W. (1986) "Fast sound in two-component liquids", *Phys. Rev. Lett.* **57**, 3277.
[3] Fernández-Perea, R., Álvarez, M., Bermejo, F.J., Verkerk, P., Roessli, B. and Enciso, E. (1998) "Collective ionic dynamics in a molten binary alloy", *Phys. Rev. E* **58**, 4568.
[4] Adams, E.M., McDonald, I.R. and Singer, K. (1977) "Collective dynamical properties of molten salts: molecular dynamics calculations on sodium chloride", *Proc. R. Soc. London A* **357**, 37.
[5] Bryk, T. and Mryglod, I. (1999) "Transverse optic-like modes in binary liquids", *Phys. Lett.* **261**, 349.
[6] Canales, M., Padró, J.A., González, L.E. and Giró, A. (1993) "Molecular dynamics simulation of liquid lithium", *J. Phys.: Condens. Matter* **5**, 3095.
[7] Jacucci, G. and McDonald, I.R. "Collective excitations in a liquid alloy", *J. Phys. F: Met. Phys.* **10**, L15.
[8] Campa, A. and Cohen, E.G.D. (1988) "Observable fast kinetic eigenmode in binary noble-gas mixtures?", *Phys. Rev. Lett.* **61**, 853.
[9] Campa, A. and Cohen, E.G.D. (1990) "Fast sound in binary fluid mixtures", *Phys. Rev. A* **41**, 5451.
[10] Anento, N. and Padró, J.A. (2000) "Longitudinal collective modes in simple liquid binary alloys: A computer simulation study", *Phys Rev. B* **62**, 11428.
[11] Anento, N. and Padró, J.A. (2001) "Molecular dynamics study of the longitudinal modes in disparate-mass binary liquid mixtures", *Phys Rev. E* **64**, 021202.
[12] Anento, N. and Padró, J.A. (2002) "Propagating density fluctuations in liquid mixtures: From hydrodynamic to molecular length scales", *J. Chem. Phys.* **116**, 6159.
[13] Balucani, U. and Zoppi, M. (1994) *Dynamics of the Liquid State* (Clarendon Press, Oxford).
[14] González, L.E., González, D.J., Silbert, M. and Alonso, J. (1993) "A theoretical study of the static structure and thermodynamics of liquid lithium", *J. Phys.: Condens. Matter* **5**, 4283.
[15] Sangster, M.J.L. and Dixon, M. (1976) *Adv. Phys.* **25**, 247.
[16] March, N.H. and Tosi, M.P. (1986) *Atomic Dynamics in Liquids* (MacMillan, London).
[17] Alcaraz, O., *Estudi de sals foses mitjançant la Dinàmica Molecular* Ph.D. Thesis, Universitat Politècnica de Catalunya.
[18] Parrinello, M., Tosi, M.P. and March, N.H. (1974) "Excitations and atomic transport in classical binary isotopic fluids", *J. Phys. C: Solid State Phys.* **7**, 2577.
[19] Giaquinta, P.V., Parrinello, M. and Tosi, M.P. (1978) "Collective dynamics of charge fluctuations in ionic conductors", *Physica*(92A), 185.
[20] Bafile, U., Verkerk, P., Guarini, E. and Barocchi, F. (2001) "Neutron brillouin scattering study of collective dynamics in a dense He–Ne gaseous mixture", *Phys. Rev. Lett.* **86**, 1019.